https://doi.org/10.5194/os-2021-84
Preprint. Discussion started: 8 September 2021

Ocean Science Discussions
Open Access

Forecasting Hurricane-forced Significant Wave Heights using the Long Short-Term Memory Network in the Caribbean Sea

Brandon J. Bethel[1], Wenjin Sun[1,2], Changming Dong[1,2,3*]

[1] School of Marine Sciences, Nanjing University of Information Science and Technology, Nanjing 210044, China

[2] Southern Ocean Science and Engineering Guangdong Laboratory (Zhuhai), Zhuhai 519000, China

[3] Department of Atmospheric and Oceanic Sciences, University of California, Los Angeles, CA 90095, USA

*Correspondence to: Changming Dong (cmdong@nuist.edu.cn)

Abstract. A Long Short-Term Memory (LSTM) neural network is proposed to predict hurricane-forced significant wave heights (SWH) in the Caribbean Sea (CS) based on a dataset of 20 CS, Gulf of Mexico, and Western Atlantic hurricane events collected from 10 buoys from 2010 – 2020. SWH nowcasting and forecasting are initiated using LSTM on 0-, 3-, 6-, 9-, and 12-hour horizons. Through examining study cases Hurricanes Dorian (2019), Sandy (2012), and Igor (2010), results illustrate that the model is well suited to forecast hurricane-forced wave heights. Forecasts are highly accurate with regard to observations. For example, Hurricane Dorian nowcasts had correlation (R), root mean square error (RMSE), and mean absolute percentage error (MAPE) values of 0.99, 0.16 m, and 2.6%, respectively. Similarly, on the 3-, 6-, 9-, and 12-hour forecasts, results produced R (RMSE; MAPE) values of 0.95 (0.51 m; 7.99%), 0.92 (0.74 m; 10.83%), 0.85 (1 m; 13.13%), and 0.84 (1.24 m; 14.82%), respectively. However, the model also consistently over-predicted the maximum observed SWHs. To improve models results, additional research should be geared towards improving single-point LSTM neural network training datasets by considering hurricane track and identifying the hurricane quadrant in which buoy observations are made.

Keywords: hurricanes; significant wave height; wave height forecasting; Long Short-Term Memory network; Hurricane Dorian; Caribbean Sea

1. Introduction

Ordinarily, momentum and mechanical energy are transferred to the ocean's surface from the overlying atmosphere, giving rise to ubiquitous surface gravity waves and other phenomena, under forcing by tropical cyclones (TC), these waves become extreme. As such, the study of TC-induced extreme significant wave heights (SWH) is at the current forefront of research and is traditionally accomplished by using an array of numerical models (Shao et al., 2019; Chao et al., 2020; Hu et al., 2020). However, although hindcasting, nowcasting, and forecasting (Alina et al., 2019; Cecilio and Dillenburg, 2020) can be

https://doi.org/10.5194/os-2021-84
Preprint. Discussion started: 8 September 2021

performed using these models, they are all disadvantaged in that they all require large investments in high-performance computing resources, technical and scientific expertise, and crucially, time. For the Small Island Developing States and coastal communities of the Caribbean Sea (CS), that have yet to significantly invest in numerical modeling capabilities, other computationally cost-effective measures are required for wave height predictions. Consequently, alternatives are high priority. Recent research into artificial intelligence (AI)-based methodologies have shown that these techniques are highly effective at forecasting wave properties with minor computational expense, even under TC-forced states (Qiao and Myers, 2020; 2021).

Demonstrating, Chen et al. (2021) constructed a random forest (RF) supervised learning classifier to generate a surrogate for the Simulating Waves Nearshore (SWAN) third-generation numerical model and reduced the required computational time by a factor of 100. Wu et al. (2020) considered a physics-based machine learning model in conjunction with an artificial neural network for predictions of SWH and peak wave period where wind forcing, and initial wave boundary conditions are considered as inputs. Campos et al. (2021) used RF to select wind and wave variables to enhance wave forecasts. They found that RF was able to select the best forecast only in very short ranges using inputs of SWH, wave direction and period. However, variable selection for longer forecasts (five days and above) was much less certain. Huang and Dong (2021) improved upon the short-term prediction of SWH by decomposing deterministic and stochastic components using a complete ensemble empirical mode decomposition (CEEMD) algorithm and recurrence quantification analysis. A similar study by Zhou et al. (2021a) demonstrated that combining EMD and the long short-term memory (LSTM) network could also reduce SWH forecasting errors in the CS.

These methods are also effective under TC conditions. Important for the present study, Chen et al. (2020) applied a machine learning method to perform probabilistic forecasting of typhoon-forced coastal wave heights and found that the model could, based on wave height data and an array of typhoon characteristics, generate the predicted confidence interval that enclosed observed wave heights. Meng et al. (2021) considered introducing a deep learning method for long-term predictions of TC-forced nearshore wave heights. The bidirectional Gated Recurrent Unit network was identified as an effective model for real-time and 24-hours ahead predictions. Wei and Cheng (2020) developed a two-step wind-wave prediction model to predict wind speed and wave height under typhoon conditions and compared results with a one-step approach. It was identified that deep recurrent neural networks could be used for forecasting in either case, but the two-step approach was more effective. Zhou et al. (2021b) used the convolutional-LSTM (convLSTM) network to predict TC-induced SWHs in the South China Sea and found that up to a 12-hour forecast horizon, the correlation between forecasted values and observations could reach 0.94.

Recently, Bethel et al. (2021) used LSTM to eliminate gaps in either surface wind speed or SWH by using one variable as a predictand to forecast its counterpart. While mean states were the focus of that study, one hurricane was used to demonstrate

https://doi.org/10.5194/os-2021-84
Preprint. Discussion started: 8 September 2021

Ocean Science Discussions

the methodology's effectiveness under extreme states. This study continues along that path to generate an LSTM-based forecast model exclusively for hurricane-forced SWHs in the CS using a set of input variables. This is deemed important for assessing and mitigating the risk of catastrophic losses in life and economic productivity due to hurricanes as seen most recently with the September 1st, 2019, landfalling of Hurricane Dorian in The Bahamas.

The remainder of this paper is structured as follows. Section 2 describes the data and methodology employed. Section 3 presents the main findings of this study. Sections 4 and 5 provide a discussion and the conclusion, respectively.

2. Data and Methodology

2.1 Observational Data

This study employs 10 buoys located throughout the CS, Gulf of Mexico, and Western Atlantic Ocean (Figure 1; Table 1) that are owned and operated by the National Data Buoy Center (NDBC; https://www.ndbc.noaa.gov/). Acquired variables include observations of surface wind speed and SWH. Gaps in buoy observations were processed using the insertion of WaveWatch III reanalysis data acquired from the Pacific Islands Ocean Observing System (https://coastwatch.pfeg.noaa.gov/). A total of twenty hurricanes identified from 2010 – 2020 were used and split into LSTM training and test datasets (Table 2). Hurricane statistics were acquired from the hurricane database maintained by the National Hurricane Center (https://www.nhc.noaa.gov/).

Table 1. List of National Data Buoy Center buoys and their statistics.

Buoy No.	Buoy ID	Latitude (°N)	Longitude (°W)	Anemometer Height (m)	Water Depth (m)
1	42002	26.055	93.64	3.8	3088
2	41010	28.878	78.485	4.1	890
3	41043	21.030	64.790	4.1	5362
4	41046	23.822	68.384	3.8	5549
5	41047	27.514	71.494	3.7	5321
6	41048	31.831	69.573	4.1	5394
7	41049	27.490	62.938	4.1	5459
8	42056	19.820	84.945	4.1	4554
9	42057	16.908	81.422	3.8	377
10	42058	14.776	74.548	3.8	4100

https://doi.org/10.5194/os-2021-84
Preprint. Discussion started: 8 September 2021

Ocean Science
Discussions

In some cases (e.g., Earl (2010), Igor (2010), Dorian (2019), Delta (2020)), the same hurricane was observed multiple times along its track. To increase the total length of the LSTM training/test sets, these data segments were arranged into a single time series. Additionally, cases such as Hurricane Humberto (2019) were explicitly excluded as swell contamination of the wave field could potentially lead to poor forecasts, despite its classification as a major hurricane, large effects on the marine environment (Avila-Alonso et al., 2021), and damage to the British overseas territory of Bermuda.

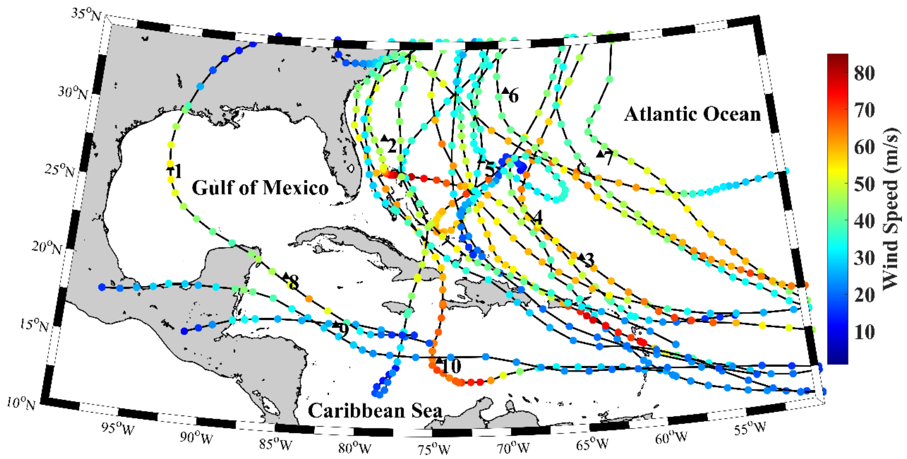

Figure 1. Geographic map of the Caribbean Sea, Gulf of Mexico, and Western Atlantic Ocean with the best-tracks of each studied hurricane and National Data Buoy Center (NDBC) buoy locations (black triangles). Numbered from 1 – 10, the NDBC buoys employed are buoys 42002, 41010, 41043, 41046, 41047, 41048, 41049, 42056, 42057, and 42058, respectively.

Table 2. Formation/dissipation dates, minimum air pressures and maximum wind speeds of the twenty hurricanes used in this study.

Dataset	Hurricane (YYYY)	Formation Date (MM/DD)	Dissipation Date (MM/DD)	Minimum Air Pressure (hPa)	Maximum Wind Speed (m/s)
Training Set	Earl (2010)	8/25	9/5	927	63.8
	Irene (2011)	8/21	8/30	942	54.16
	Katia (2011)	8/29	9/12	942	61.1
	Ernesto (2012)	8/1	8/10	973	43
	Cristobal (2014)	8/23	9/2	965	38.8
	Gonzalo (2014)	10/12	10/20	940	63.8
	Bertha (2014)	8/1	8/16	998	36.1
	Joaquin (2015)	9/28	10/15	931	69.4
	Matthew (2016)	9/27	10/7	934	75
	Jose (2017)	9/5	9/25	938	69.4

https://doi.org/10.5194/os-2021-84
Preprint. Discussion started: 8 September 2021

	Maria (2017)	9/16	10/2	908	77
	Irma (2017)	8/30	9/14	914	79.16
	Florence (2018)	8/31	9/18	937	66.6
	Nana (2020)	9/1	9/4	994	33.3
	Teddy (2020)	9/12	9/24	945	66.1
	Delta (2020)	10/4	10/12	953	61.1
	Isaias (2020)	7/30	8/5	986	41.6
Test Set	Dorian (2019)	8/24	9/7	910	82.7
	Sandy (2012)	10/22	11/2	940	51.38
	Igor (2010)	9/8	9/23	924	69.4

2.2 Methodology

2.2.1 The Long Short-Term Memory Network

Originally developed by Hochreiter and Schmidhuber (1997), the LSTM network belongs to a class of recurrent neural networks (RNNs). Along with its variants, LSTM has been widely used in forecasting and data reconstruction studies (Kim et al., 2020; Bethel et al., 2021; Gao et al., 2021; Hu et al., 2021; Jörges et al., 2021). It has also been coupled with other machine learning tools, neural networks, and numerical models (Choi and Lee, 2018; Ali and Prasad, 2019; Fan et al., 2020; Guan, 2020). LSTMs have an advantage over traditional feed-forward neural networks and other RNNs in that they can selectively remember patterns in data. This is achieved by a series of forget (f_t), input (i_t), and output (o_t) gates. Data passing through these gates are processed using the sigmoid function (σ) and the Hadamard product operator ($\odot$; Yu et al., 2019). Each gate may be computed as follows:

$$f_t = \sigma\left(W_{xf}x_t + W_{hf}h_{t-1} + b_f\right) \quad (1)$$

$$i_t = \sigma(W_{xi}x_t + W_{hi}h_{t-1} + b_i) \quad (2)$$

$$o_t = \sigma(W_{xo}x_t + W_{ho}h_{t-1} + b_o) \quad (3)$$

$$g_t = tanh\left(W_{xg}x_t + W_{hg}h_{t-1} + b_g\right) \quad (4)$$

$$c_t = f_t \odot c_{t-1} + i_t \odot g_t \quad (5)$$

$$h_t = o_t \odot tanh(c_t) \quad (6)$$

where W is each layer's assigned weight, x_t is the input time step t, b is the bias, c is the cell state, and tanh is a hyperbolic tangent function.

https://doi.org/10.5194/os-2021-84
Preprint. Discussion started: 8 September 2021

Ocean Science
Discussions

In sequence, the forget gate is used to delete past information where decisions on which information should be deleted is defined as the value obtained from estimating the sigmoid following receiving h_{t-1} and x_t. The sigmoid function output ranges from 0 to 1 so that if the value is 0, information of the previous state is completely deleted, and if 1, information is completely preserved. The input gate saves current information and is processed alongside h_{t-1} and x_t before being applied to the sigmoid function. The resulting information is then processed with the hyperbolic function and Hadamard product operator before being sent out of the input gate. The strength and direction of information storage in the current cell is represented by i_t and g_t, which respectively range from 0 to 1, and -1 to 1.

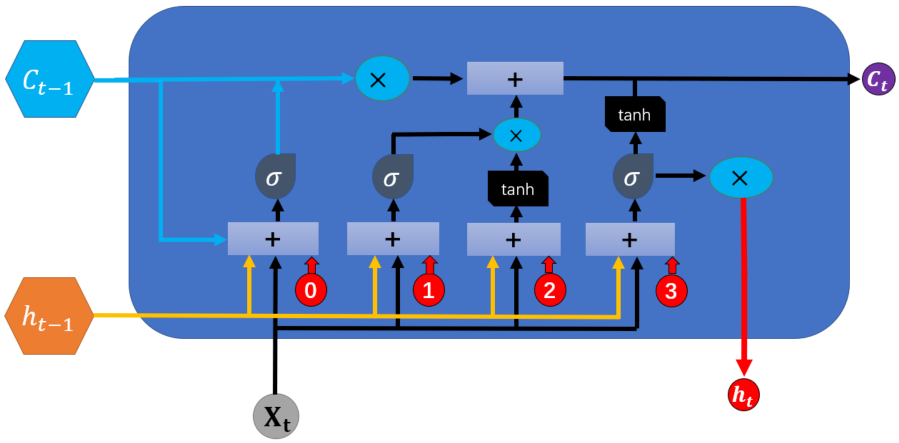

Figure 2. Architecture of the long short-term memory neural network cell.

LSTM is set up with four layers that correspond to a time step of 4. The recursive linear unit (ReLu) was used as the activation function to maximize the model's ability to capture nonlinearities. The data was partitioned along a 70/30 split into training and validation datasets. The number of epochs was set to 100 and the batch size set to 1. Throughout each experiment, the operating parameters were held constant.

2.2.2 Wind Speed Extrapolation

As seen in Table 1, no buoy measured wind speed at the standard 10 m height and thus, wind speeds were adjusted to this height using the logarithmic wind profile:

$$U_{10} = U_x \frac{\ln(10/Z_0)}{\ln(x/Z_0)} \tag{7}$$

where U_x is the wind speed measured at a given buoy's anemometer height, x is a given buoy's anemometer height, and Z_0 is the roughness length (0.0002; Golbazi and Archer, 2019).

2.2.3 Performance Indicators

Three commonly used statistical metrics: correlation coefficient (R), root mean square error (RMSE), and mean absolute

https://doi.org/10.5194/os-2021-84
Preprint. Discussion started: 8 September 2021

Ocean Science
Discussions

percentage error (MAPE), are used to assess forecast efficacy. Their equations are as follows:

$$R = 1 - \frac{\sum_{i=1}^{N_i}(x_i - \dot{x}_i)^2}{\sum_{i=1}^{N_i}(x_i - \bar{x}_i)^2}$$

$$RMSE = \sqrt{\frac{\sum_{i=1}^{N_i}(x_i - \dot{x}_i)^2}{N_i}} \tag{8}$$

$$MAPE = \frac{1}{N_i}\sum_{i=1}^{N_i}\left|\frac{|x_i - \dot{x}_i|}{x_i}\right| \times 100\%$$

where x_i and $\dot{x}_i$ are the observed and forecasted SWH (m), respectively. N_i is the total number of observations and the overbar denotes averages.

3. Results

3.1 Time Series Analysis

To evaluate forecast efficacy, time series of the observed and LSTM-forecasted, hurricane-forced SWHs for Hurricanes Dorian, Sandy, and Igor are given in Figures 3 – 5, respectively. Due to the lack of nearshore buoy observations within The Bahamas, no observations were made when Hurricane Dorian made landfall on Abaco island on September 1st, 2019. NDBC buoy 41010 nevertheless observed the growth of SWH under the influence of the hurricane several hundred kilometres away. In Fig. 3, time series of observed SWH was compared with the nowcast (0-hour, Fig. 3(a) and 3-, 6-, 9-, and 12-hour forecasts (Fig. 3b-e, respectively). In Fig. 3a, it can be observed that an extremely tight fit between the forecasts and observations of Hurricane Dorian-forced SWHs at the start of wave growth from ~3.5 m to just under 7 m. However, at closer inspection, it can also be seen there are periods (e.g., at 42-hours after UTC 1500 September 1) where the LSTM nowcast is unable to capture the extremely fine details. Nevertheless, this represents a discrepancy of far less than 1 m and is thus of very little importance when considering estimates of the wave state. When forecasts are performed on a 3-hour horizon, however, discrepancies between observations and the forecast have grown significantly larger where at different times, forecasted SWHs both underestimate and overestimate the observations. This phenomenon is especially noticeable at the 40- and 50-hours after UTC 1500 September 1 marks. At the 40-hour mark, SWHs were observed by buoy 41010 at approximately 5.5 m, but LSTM predicted a height of only approximately 4.2 m. The difference between the two clearly exceeds 1 m.

https://doi.org/10.5194/os-2021-84
Preprint. Discussion started: 8 September 2021

Ocean Science Discussions
Open Access
EGU

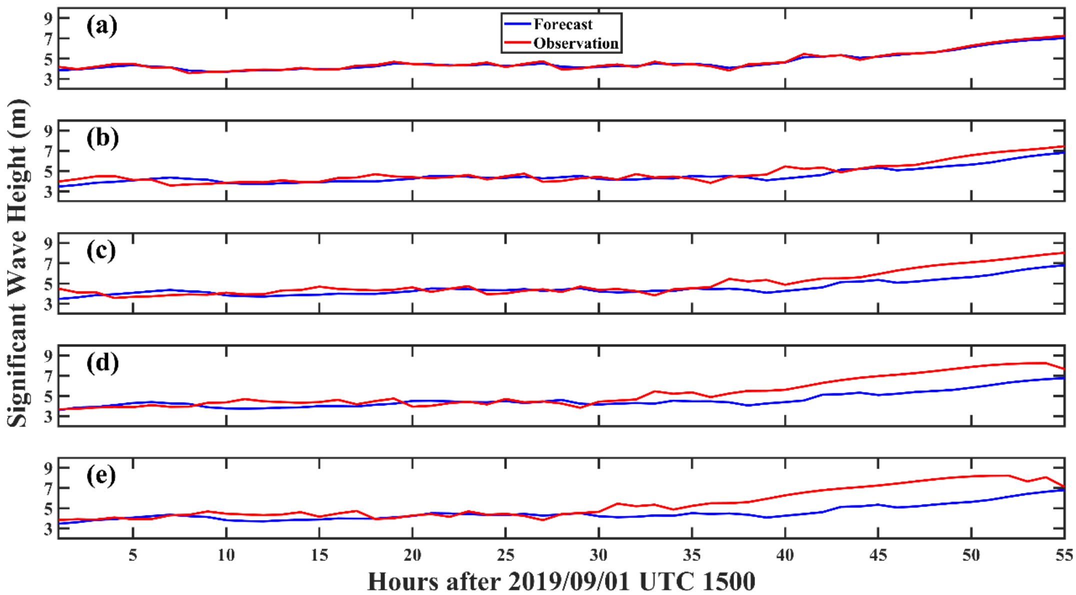

Figure 3. Time series of Hurricane Dorian observed and LSTM-forecasted SWH (m) at the (a) 0-, (b) 3-, (c) 6-, (d) 9-, and (e) 12-hour horizons, measured at buoy 41010.

As total wave energy (P) is extremely sensitive to SWH (i.e., $P \propto H_s^2 T_p$, where H_s is the SWH and T_p is the wave period), even minor underestimations of the wave height would lead to radically different energy output. Similarly, at the 50-hour mark, SWH was measured at approximately 5.6 m, but LSTM forecasted a wave height of approximately 6.5 m. This overestimation would produce the same radically different energy output than the observations. The same phenomenon can still be observed for the 6-, 9- and 12-hour forecast horizons respectively presented in Fig. 6c-e, but at a significantly exacerbated scale. In each case, at the tail end of the forecasts (35+ hours after UTC 1500 September 1), the distance between the observations and forecasts widened as the maximum wave height increased.

Identical to Hurricane Dorian, nowcasts of Hurricane Sandy were most efficient at reproducing the observations (Fig. 4a). Interestingly, though there are some slight differences, LSTM was still able to capture finescale increases or decreases in SWH. As the forecast horizon is extended to 3-hour in Fig. 4b, however, those finescale details were increasingly missed, though the general wave growth and decay trends were captured. In Fig. 4c for the 6-hour forecast horizon, and before the 40-hours after UTC 2000 September 10 mark, LSTM nearly consistently underestimated wave heights, but this was minor. Following this point at the peak of the storm, LSTM virtually captured the observed SWH although finescale details were completely missed. During the wave height decay stage, LSTM-forecasted wave heights overestimated the observations, but this discrepancy hovered at ~0.5 m and so, were not as extreme as the discrepancies seen during Hurricane Dorian at the same 6-hour forecast horizon (Fig. 3c). In Fig. 4d and 4e where the 9- and 12-hour forecast horizons are compared with observations, the differences

https://doi.org/10.5194/os-2021-84
Preprint. Discussion started: 8 September 2021

between them is significantly larger than as compared to the 0-hour nowcast or the 3- and 6- hour forecast horizons of Fig. 4a-c.

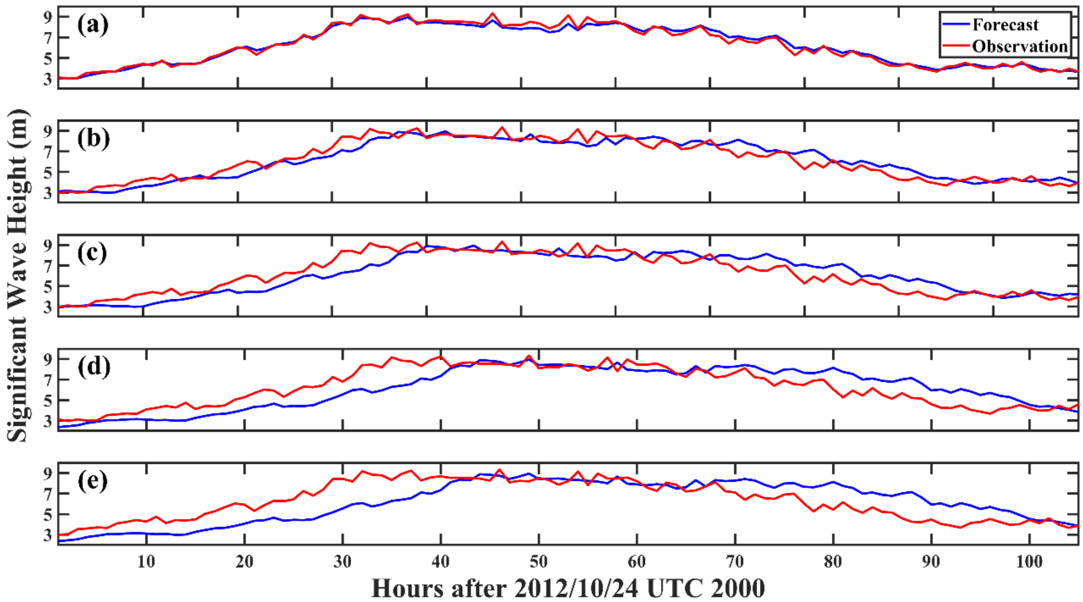

Figure 4. Same as Figure 3, but for Hurricane Sandy (2012) measured at buoy 42058.

At its most extreme, the difference between the forecasted (~6 m) and observed (~9 m) SWH reached a staggering 3 m at the 32-hour mark after UTC 2000 October 24. However, eight hours later at the peak of the storm, LSTM was once again able to predict the observed SWHs more adequately. Although LSTM was able to capture the general decreasing, it largely overestimated the SWH as wave heights began to decrease with the passing of the storm. This overestimation was measured at approximately 2 m at the 90-hour mark after UTC 2000 October 24.

Although Hurricanes Dorian and Sandy, like Hurricane Igor, were extremely powerful systems, Igor however, spent the majority of its time in the Atlantic Ocean far away from any landmasses. Perhaps, then, the maximum wave height was allowed to grow to just under 11 m as an extremely long, uninterrupted fetch and duration would have been conducive for this wave growth. This is, of course, tempered by wind energy transfer rates and energy saturation of the wave field (Liu et al., 2008; Hwang and Fan, 2017; Babanin et al., 2019), in addition to balancing and decay by dissipative forces (Allahdadi et al., 2019; Rollano et al., 2019; Tamizi et al., 2021). In Fig. 5, similar to the previous two examples, the LSTM nowcast (Fig. 5a) produced exceptionally accurate results for Hurricane Igor (2010) with regards to the observations.

https://doi.org/10.5194/os-2021-84
Preprint. Discussion started: 8 September 2021

Ocean Science
Discussions

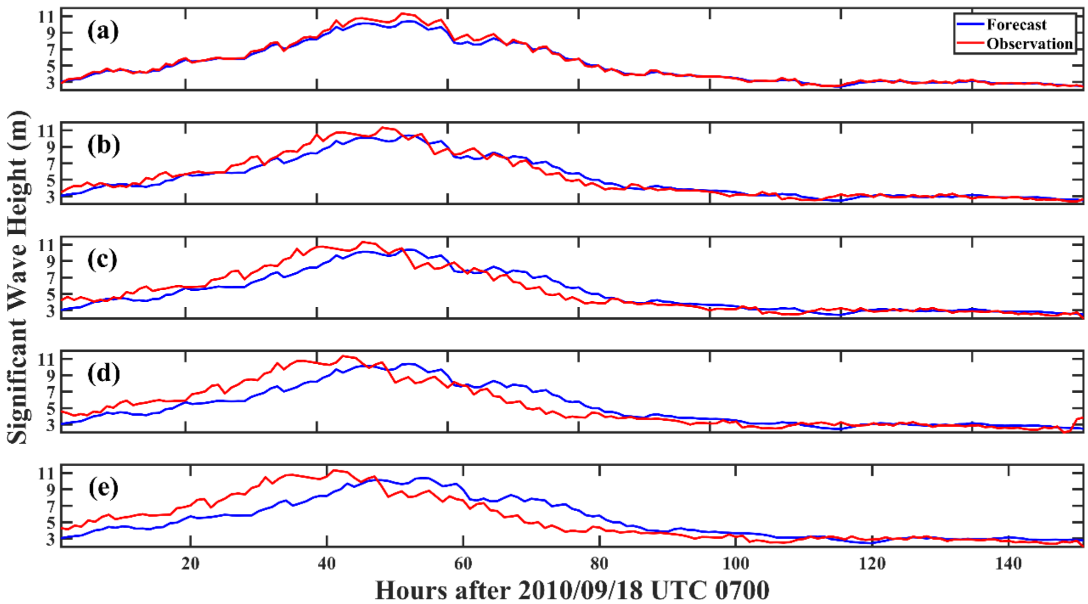

Figure 5. Same as Figure 3, but for Hurricane Igor (2010) measured at buoys 41048 and 41049.

This is even true at the peak of the storm at the 50-hour mark after UTC 0700 September 18 when wave heights reached a maximum of just under 10 m. As the forecast horizon increased, however, the same pattern of forecast quality deterioration could be observed where in Fig. 5b at the 3-hour horizon. Although LSTM was able to capture the general trend throughout the time series, LSTM's predictions were slightly out of phase with the observations in its estimation of the point at which the storm generated its maximum wave height (50 hours after UTC 0700 September 18). This phenomenon becomes increasingly apparent in the 6-hour (Fig. 5c), 9-hour (Fig. 6d) to the 12-hour (Fig. 5e) forecast horizons. Nevertheless, at the tail end of the time series, regardless of the forecast horizon, LSTM produced highly accurate predictions of SWH under forcing by Hurricane Igor (2010).

3.2 Histogram Analysis

Precise and not merely accurate estimates of hurricane-forced SWHs have the potential to enhance risk assessments and mitigation strategies as these systems make landfall or approach offshore structures (Hatzikyriakou and Lin, 2017; Marsooli and Lin, 2018; Masoomi et al., 2018; Guo et al., 2020; Song et al., 2020). This first section investigates the distribution of forecasted SWHs in comparison with observations for hurricanes Dorian, Sandy, and Igor. In Fig. 6, histograms of observed and forecasted SWHs under forcing by Hurricane Dorian is presented. In Fig. 6a, it can be observed that for the 0-hour SWH nowcast, the model is able to completely reproduce wave heights ranging from 3 – 4 m, but with higher waves, the model's ability gradually deteriorates with regards to frequency predictions. Specifically, at the 4 – 4.5 m range, the model underestimates the observations, but this pattern alternates to overestimates the observation with subsequent 0.5 m bins. The

https://doi.org/10.5194/os-2021-84
Preprint. Discussion started: 8 September 2021

model also completely overestimated the maximum wave height, providing results for wave heights at the 8 – 9 m range, though there are no observed occurrences. At longer forecast horizons, the lowest wave heights (3 – 4.5 m) were consistently underestimated in terms of frequency, but an alternating pattern of over- and underestimations follow in subsequent bins. In Fig. 6b, relatively good agreement between the forecasted and observed SWHs, but discrepancies between them have become increasingly apparent. This is especially noticeable at the 4 – 4.5 m wave height range where there were LSTM underestimations, and in the next 5 – 5.5 m range, the model overestimated the observations. The trend remains consistent for the 6-, 9-, and 12-hour forecast horizons presented in Fig. 6c, S1, and 6d. Underestimations observed previously have become more severe, and the quantity of overestimations have increased. Identical to the nowcast of Fig. 6b, the 3-, 6-, and 12-hr forecasts overestimate the frequency of waves higher than 8 m.

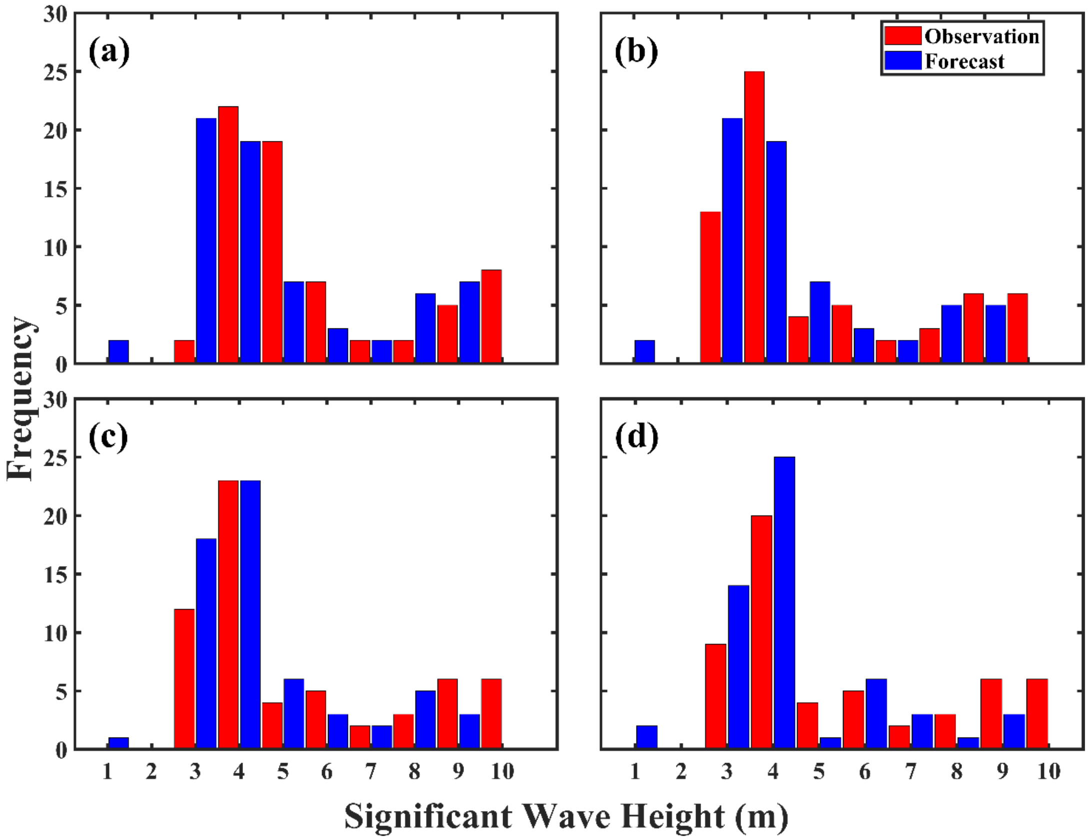

Figure 6. Histograms of Hurricane Dorian observed (blue) vs forecasted (red) SWH (m) at the (a) 0-, (b) 3-, (c) 6-, and (d) 12-hour forecast horizons. Results for the 9-hour forecast are presented in Figure S1.

Figure 7 presents histograms of observed and nowcasted/forecasted SWHs as forced by Hurricane Sandy. In Fig. 5a, while the maximum wave heights forced by Hurricane Sandy (9 m) exceeded that of Hurricane Dorian (8 m), LSTM was still able

https://doi.org/10.5194/os-2021-84
Preprint. Discussion started: 8 September 2021

to adequately predict the wave height distribution. However, alternating patterns of under- and overestimations of the frequency of wave heights can still be observed, with this becoming more severe over time at the 3-, 6-, and 9-hour forecast horizons presented in Fig. 7b, S2, and 7c. At the 12-hour horizon in Fig. 7d, the lowest wave heights were nearly completely missed by LSTM, but with increasing heights, the model began to overestimate the frequency of the observations. A consistent feature of the model is its apparent overestimation of both the frequency of wave heights, and its magnitude. Specifically, the model predicts wave heights that are approximately 1 m higher than the total. This may indicate that the training dataset contains too many examples of very high wave heights, which thus necessities the inclusion of less powerful hurricanes for model training.

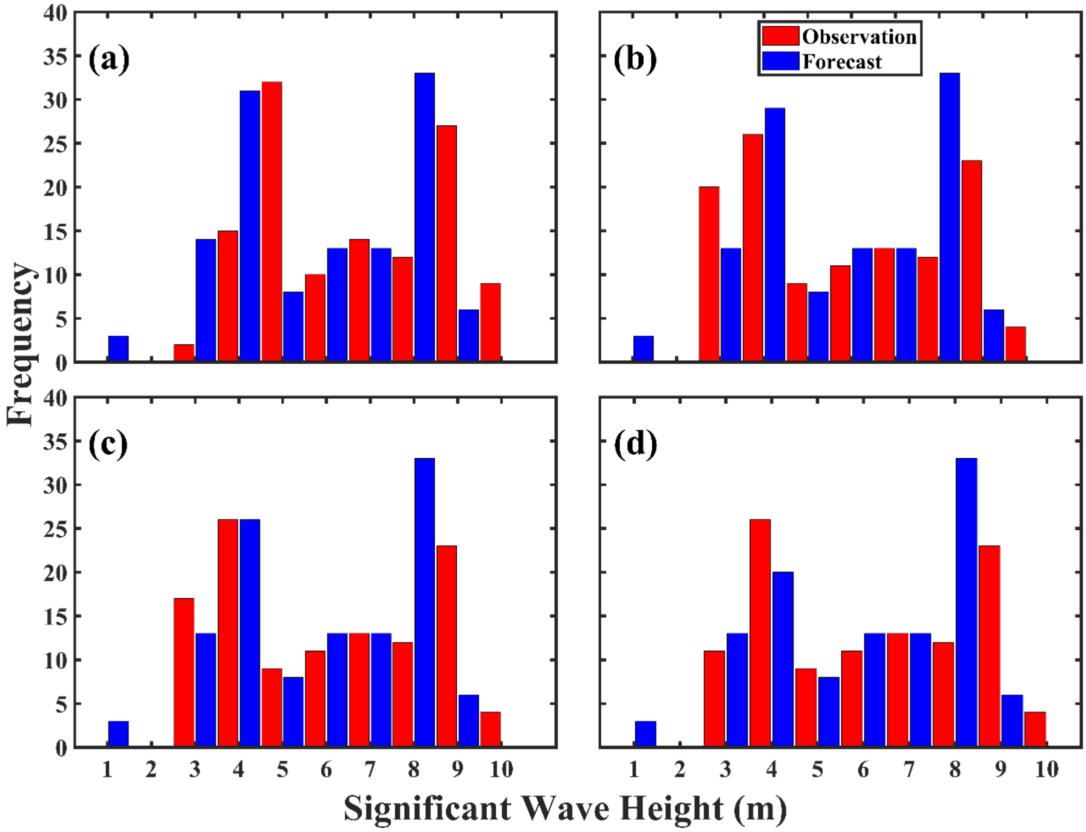

Figure 7. Same as Figure 6, but for Hurricane Sandy. Results for the 9-hour forecast are presented in Figure S2.

Results for Hurricane Igor are presented in Fig. 8. Here, Igor produced SWHs that exceeded either Hurricanes Dorian or Sandy, but interestingly, regardless of the forecast horizon, LSTM was able efficiently (but still imperfectly) forecast the wave height distribution, even at wave heights up to 10.5 m. This was previously not observed for either Hurricanes Dorian (Fig. 6) or Sandy (Fig. 7). However, identical to the previous hurricane cases, the frequency of maximum wave height predictions (10.5 – 12 m) are overestimated. Throughout the forecast horizons, naturally, the 0-hour forecast produced the best results (Fig. 8a).

https://doi.org/10.5194/os-2021-84
Preprint. Discussion started: 8 September 2021

Ocean Science
Discussions
Open Access

Deterioration of the forecasted wave height frequency and magnitude increased steadily from the 3-, 6-, 9-, and 12-hour forecast horizons in Fig. 8b-c, S3, and 8d.

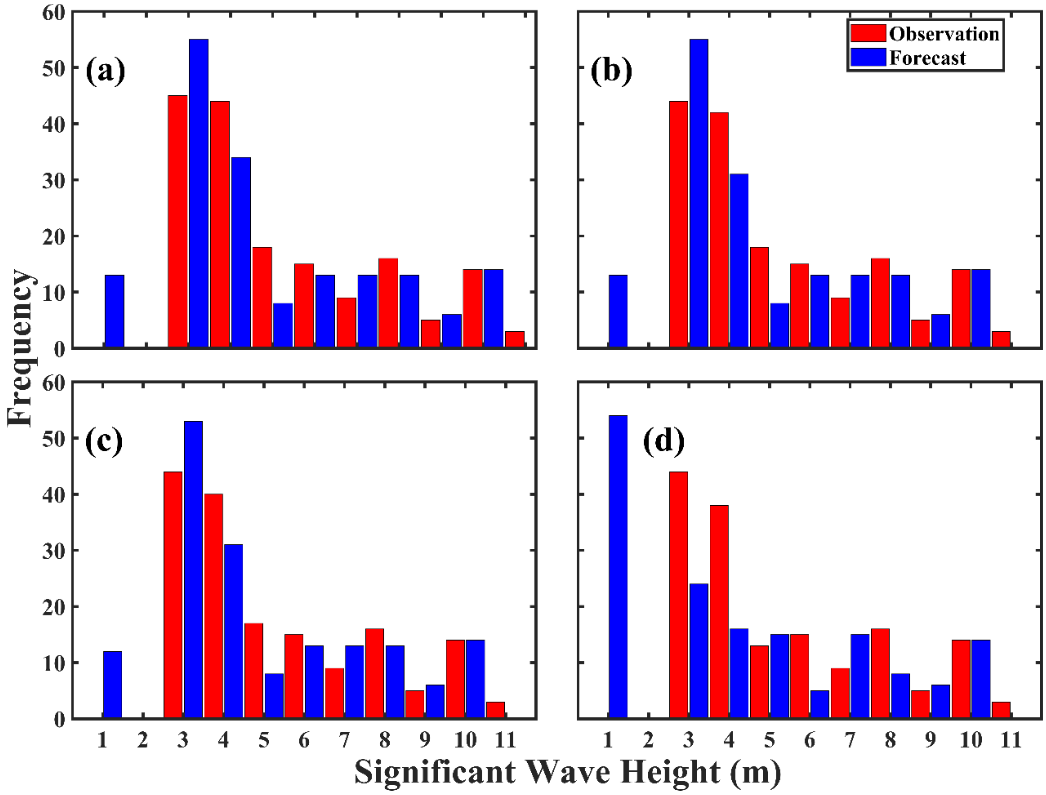

Figure 8. Same as Figure 6, but for Hurricane Igor (2010). Results for the 9-hour forecast are presented in Figure S3.

3.3 Total Model Performance

Overall forecast quality can be assessed through the statistical metrics of R, RMSE, and MAPE. Results for R and RMSE for each hurricane are illustrated graphically in Fig. 9. Results for MAPE for all three hurricanes are presented in Fig. 10. The full range of statistics is available in Table 3. In Fig. 9, it can be observed model forecast effectiveness deteriorated over time but in the 0 – 6-hour time frames, the R remained above 0.9 and the RMSE was under 0.8 m. After this point, however, R decreased to a minimum of 0.84 and RMSE reached a maximum of 1.24 m beyond the 9-hour horizon to the 12-hour horizon. This demonstrates that the model remained highly effective at predictions over a 12-hour time frame. Similarly, with regards to Hurricane Sandy, it can be observed that R also decreased and RMSE increased gradually over increasing forecast horizons, but results were largely poorer than Hurricane Dorian's at the 12-hour forecast horizon. For Hurricane Igor, results were more similar to the Hurricane Dorian case. It can be seen that the R decreased from an initial value of 0.99 and an RMSE of 0.29 m at the 0-hour nowcast, to 0.96 and 0.66 m at the 3-hour forecast, and then again to 0.93 and 0.95 at the 6-hour forecast. Crucially,

https://doi.org/10.5194/os-2021-84
Preprint. Discussion started: 8 September 2021

within the 9-hour forecast window, RMSEs were measured at 1 m or lower. However, at the 12-hour forecast horizon, R decreased to 0.82, while the RMSE increased by a factor of ~1.5 to 1.52 m. At the same forecast horizons, Hurricane Igor results outperform Hurricane Sandy's.

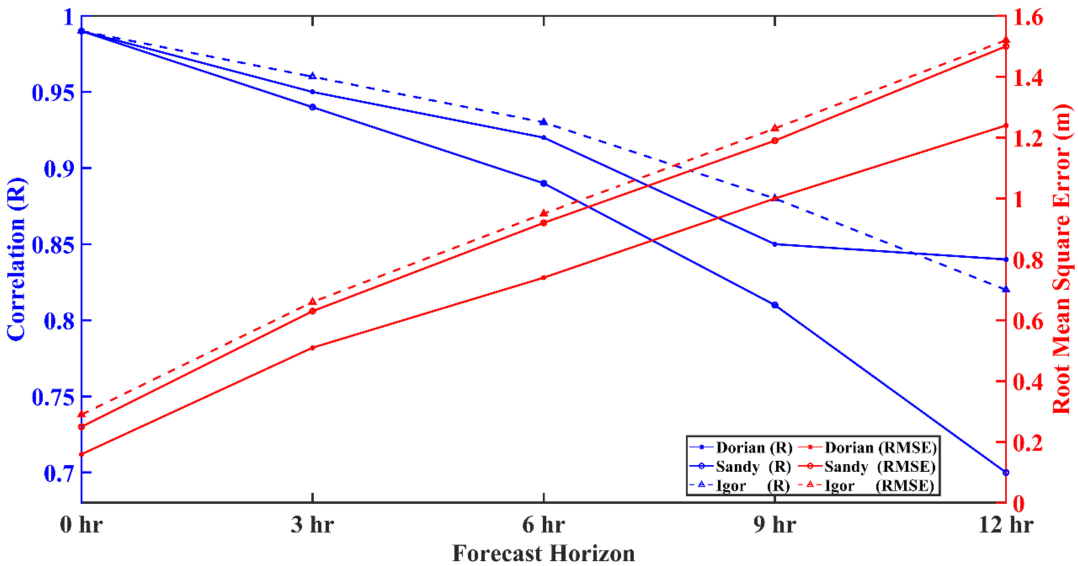

Figure 9. LSTM model forecast performance in terms of R (blue) and RMSE (red) as compared with the observations for Hurricane Dorian.

In Fig. 10, the MAPE for each of the hurricanes are given. There, it can be observed that regardless of forecast horizon, Dorian produced the lowest MAPE values out of the three case studies, followed by Sandy and then Igor. Specifically, Hurricane Dorian had MAPE values of 2.6% at the 0-hour nowcast and values of 7.99%, 10.83%, 13.13%, and 14.82% respectively at the 3-, 6-, 9-, and 12-hour forecast horizons. By contrast Hurricanes Sandy (Igor) had MAPE values of 3.41% (3.36%), 9.15% (9.53%), 13.34% (13.78%), 17.55% (17.70%), and 22.08% (21.88%) at the 0-, 3-, 6-, 9-, and 12-hour forecast horizons. Both Hurricanes Sandy and Igor had MAPE values approximately 67% higher than that of Hurricane Dorian at the 12-hour horizon. Although the reason for this is unclear, it may be related to any set of factors ranging from the properties inherent to Dorian itself (e.g., it's extremely slow translation speed of ~1.4 – 2 m/s) or its landfalling environment (Sahoo et al., 2019).

https://doi.org/10.5194/os-2021-84
Preprint. Discussion started: 8 September 2021

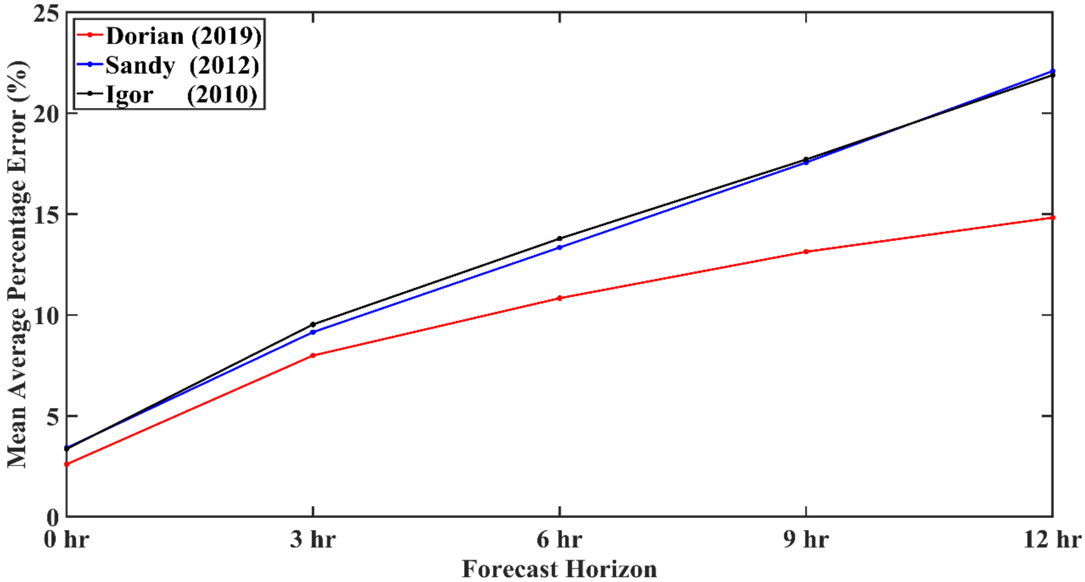

Figure 10. Mean average percentage error (%) for Hurricanes Dorian (red), Sandy (blue), and Igor (black).

In summary, Dorian now- and forecasts resulted in R (RMSE; MAPE) values of 0.99 (0.16 m, 2.6%), 0.95 (0.51 m; 7.99%), 0.92 (0.74 m; 10.83%), 0.85 (1 m; 13.13%), and 0.84 (1.24 m; 14.82%), for the 0, 3, 6, and 12 forecast horizons, respectively. Hurricane Sandy SWH forecasts resulted in R (RMSE; MAPE) values of 0.99 (0.25 m; 3.14%), 0.94 (0.63 m; 9.15%), 0.89 (0.92 m; 13.34%), 0.81 (1.19 m; 17.55), and 0.70 (1.51 m; 22.08%) at the 0-, 3-, 6-, 9-, and 12-hour forecast horizons, respectively. Hurricane Igor SWH forecasts produced R (RMSE; MAPE) values of 0.99 (0.29 m; 3.36%), 0.96 (0.66 m; 9.53%), 0.93 (0.95 m; 13.78%), 0.88 (1.52m; 17.70%), and 0.82 (1.52 m; 21.88%), for the 0-, 3-, 6-, 9-, and 12-hour forecast horizons, respectively.

https://doi.org/10.5194/os-2021-84
Preprint. Discussion started: 8 September 2021

Table 3. LSTM forecast performance for Hurricanes Dorian, Sandy, and Igor.

	R					RMSE (m)					MAPE (%)				
	Forecast Hour					Forecast Hour					Forecast Hour				
	0	3	6	9	12	0	3	6	9	12	0	3	6	9	12
Dorian	0.99	0.95	0.92	0.85	0.84	0.16	0.51	0.74	1.00	1.24	2.6	7.99	10.83	13.13	14.82
Sandy	0.99	0.94	0.89	0.81	0.70	0.25	0.63	0.92	1.19	1.51	3.14	9.15	13.34	17.55	22.08
Igor	0.99	0.96	0.93	0.88	0.82	0.29	0.66	0.95	1.23	1.52	3.36	9.53	13.78	17.70	21.88

4. Discussion

Forecasting hurricane activity and its properties remains a daunting task for the scientific community, but great strides have been made in the development of statistical/probabilistic methods, numerical models, and as presented in this study, AI techniques. The results of this study are in strong agreement with those observed by Meng et al. (2021) and Wei (2021) that each found that AI was highly effective at predicting hurricane-induced SWHs. However, although contemporary applications of AI in the forecasting of both in mean and extreme (i.e., TC-forced) waves states have relied traditionally on singular inputs of SWH (Ali and Prasad, 2019; Zhao and Wang, 2018; Zhou et al., 2021a, b), a growing body of literature have demonstrated that the addition of other variables such as wind speed (as done here), wind direction and other variables improves forecast effectiveness (Kaloop et al., 2020; Zubier, 2020; Raj and Brown, 2021; Wang et al., 2021). Uncertainties in variable selection have also stimulated research into how to best identify predictors for the SWH or other predictands (Li and Liu, 2020; Li et al., 2021). These results nevertheless remain consistent with the findings of Chen and Wang (2020) where the introduction of meteorological data could improve wave forecasts, but longer forecast horizons led to underestimations of extreme wave heights.

Additionally, discrepancies in forecasting outcomes between hurricanes in this study are slight, but noticeable. This may reflect differences in LSTM training and test hurricane properties. These include hurricane wind field, translation speed, approach angle and track which have been demonstrated to be essential factors in governing wave evolution (Zhang and Oey, 2018; Zhang and Li, 2019; Wang et al., 2020). For example, as a hurricane translated through the study area, wave properties in any of the four quadrants could have been measured by the chance intersection of the hurricane and its observing buoy (Zhang and Oey, 2018; Tamizi and Young, 2020; Tian et al., 2020; Collins et al., 2021). Additional variables to consider, especially in the case of those hurricanes in the CS given its numerous islands, are the morphology of those islands as they can have a strong influence on local ocean dynamics (Cheriton et al., 2021). For those hurricanes that made landfall in The Bahamas, additional consideration should be given to the nonlinear interactions that hurricane waves and storm surge have on the archipelago's narrow and steep carbonate shelf and its variability due to elongated coastlines (Sahoo et al., 2019). These can perhaps be dealt with by the special application of a combination of a high order spectral method with Krylov subspace techniques as pioneered by Köllisch et al. (2018). Another set of examples come from Puerto Rico and the U.S. Virgin Islands (Joyce et al., 2019), and the shallow continental shelf between India and Sri Lanka (Sahoo et al., 2021). Consequently, training and test datasets certainly contain data from any of a hurricane's four quadrants, or in the case of Hurricanes Joaquin (2015) and Dorian data recorded along The Bahamas' vulnerable, eastern-most, Atlantic Ocean-facing islands. In these terms, the effect of training data selection on overall forecast quality has yet to be quantified and should be assessed. Following this, finescale LSTM-based hurricane-forced SWH forecast models for a given CS country or territory could potentially benefit from increased discrimination in selecting hurricane training data.

Accompanying increased scrutiny in building LSTM training datasets to improve predictions, the usage of physics-based/informed/infused versions of LSTM and other artificial intelligence and machine learning algorithms (Karniadakis et al., 2021; Zhang et al., 2021) may help to bridge the gap in forecasting efficacy between physics-based third-generation numerical wave models such as WaveWatch III or SWAN. Crucially, this will ensure that forecasting remains significantly computationally cheaper than the usage of wave models. These methods have been successfully applied to the solving of differential equations in engineering (Niaki et al., 2021; Zobeiry, and Humfeld, 2021), analyzing blood flow (Arzani et al., 2021), and chaotic systems (Khodkar and Hassanzadeh, 2021). Relevant for the current discussion, these methods are also finding use in weather and climate modelling (Kashinath et al., 2021). Considering the large physical complexities in wave evolution under TC forcing (Tamizi et al., 2021), and the many nonlinearities that govern crucial processes (Yim et al., 2017; Constantin, 2018; Sharifineyestani and Tahvildari, 2021), incorporating physics-informed, or knowledge-guided machine learning should, respectively, improve and lengthen forecast efficacy and horizons.

5. Conclusion

Precise, computationally cheap, and rapid SWH forecasting under hurricane forcing is of immense value to safeguard lives, property, and economic development in coastal communities and especially, SIDS. This study used surface wind speed and SWH forced by 17 hurricanes as input to the LSTM neural network to nowcast and forecast SWHs in the CS. Three hurricanes, Dorian (2019), Sandy (2012), and Igor (2010) were used as test cases. Results illustrated that the model was

https://doi.org/10.5194/os-2021-84
Preprint. Discussion started: 8 September 2021

highly accurate at reproducing observed hurricane-forced wave height distributions both in terms of magnitude and frequency. However, there were discrepancies between observations and predictions. This was most easily observable from the comparison of observed and forecasted SWH time series for the three test cases.

In all cases, although the nowcasts naturally produced the best results, instances of slight under- and overestimations could nevertheless be observed at many finescale details. These under- and overestimations became more severe with increasing forecast horizon length. It has been demonstrated that wave height nowcasting (i.e., a forecast horizon of 0-hour) was very effective where in the test cases of Hurricanes Dorian (2019), Sandy (2012), and Igor (2010), R (RMSE) was measured at 0.99 (0.16 m), 0.99 (0.25 m), and 0.99 (0.29 m), respectively. Corresponding values of MAPE for Dorian, Sandy, and Igor were measured at 2.6%, 3.14%, and 3.36%, respectively. For forecast horizons ranging from 3-, 6-, 9-, and 12-hours, with regards to observations, Dorian predictions produced R (RMSE; MAPE) values of 0.95 (0.51 m; 7.99%), 0.92 (0.74 m; 10.83%), 0.85 (1 m; 13.13%) and 0.84 (1.24 m; 14.82%), respectively. Similarly, with regards to observations, Sandy predictions produced R (RMSE; MAPE) values of 0.94 (0.63 m; 9.15%), 0.89 (0.92 m; 13.34%), 0.81 (1.19 m; 17.55%) and 0.70 (1.51 m; 22.08%), respectively. Igor predictions produced R (RMSE; MAPE) values of 0.96 (0.66 m; 9.53%), 0.93 (0.95 m; 13.78%), 0.88 (1.23 m; 17.70%) and 0.82 (1.52 m; 21.88%), respectively.

This study is limited in two significant ways. Firstly, identical to Meng et al. (2021), this study focused on forecasting hurricane-forced SWHs, rather than mean states. Consequently, despite the large number of hurricanes over the study period, a minority of these hurricanes were observed by buoys. Thus, the LSTM training datasets were severely limited in hurricane cases, thus reducing forecast horizons and overall forecasting efficacy. A significantly expanded array of observational platforms in the Caribbean (i.e., both in situ buoys and remote sensing high-frequency coastal radars) would increase the likelihood of crucial hurricane wind/wave properties being observed in sufficiently high resolutions to make future research such as this possible. Secondly, and perhaps more importantly, as TCs and their properties rapidly evolve in space and time (Leroux et al., 2018; Bhalachandran et al., 2019; Chen et al., 2021), they naturally have great implications on the properties of waves they excite (Haryanto et al., 2021). If these properties change rapidly enough, LSTM alone would be unable to capture their characteristics. A recent study by Zhou et al. (2021b) demonstrated that an integrated EMD-LSTM model is more effective at forecasting rapidly evolving and large wave heights, but whether this remains true for hurricane-forced waves remains to be seen. Future research should investigate the efficacy of the EMD-LSTM model in forecasting hurricane-forced wave heights, and a ConvLSTM model fed with high-resolution wave data should be employed for two-dimensional hurricane-forced SWH.

Data Availability: Buoy datasets are provided by the National Data Buoy Center and can be accessed at https://www.ndbc.noaa.gov/. Hurricane statistics can be acquired from the National Hurricane Center at https://www.nhc.noaa.gov/. WaveWatch III reanalysis data as provided by the Pacific Islands Observing System can be acquired at https://coastwatch.pfeg.noaa.gov/.

Author Contributions: BJB, WJS and CD designed the experiments and BJB carried them out. BJB developed the model code and performed the simulations. BJB prepared the manuscript with contributions from all co-authors.

Acknowledgements: The National Data Buoy Center is greatly thanked for the continued maintenance of its buoy array in the Caribbean and for ensuring the public accessibility of its data. The National Hurricane Center is thanked for providing the hurricane statistics and the Pacific Islands Ocean Observing System is thanked for providing WaveWatch III reanalysis data.

Funding: This work was supported by the Southern Marine Science and Engineering Guangdong Laboratory (Zhuhai) (SML2020SP007), and the National Key Research and Development Program of China (2017YFA0604100, 2016YFC1402004 and 2017YFC1404200).

Competing Interests: The authors declare that they have no conflict of interest.

References

Ali, M., and Prasad, R.: SWH forecasting via an extreme learning machine model integrated with improved complete ensemble empirical mode decomposition, Renew. Sustain. Energy Rev., 104, 281-295, https://doi.org/10.1016/j.rser.2019.01.014, 2019.

Alina, A.I., Rusu, L., Catalin, A: Nearshore Wave Dynamics at Mangalia Beach Simulated by Spectral Models, J. Mar. Sci. Eng., 7(7), 206, https://doi.org/10.3390/jmse7070206, 2019.

Allahdadi, M.D., He, R., Neary, V.S: Predicting ocean waves along the US east coast during energetic winter storms: sensitivity to whitecapping parameterizations, Ocean Sci., 15(3), 617-715, https://doi.org/10.5194/os-15-691-2019, 2019

Arzani, A., Wang, J., D'Souza, R.M: Uncovering near-wall blood flow from sparse data with physics-informed neural networks, Physics of Fluids, 33(7): 071905, https://doi.org/10.1063/5.0055600, 2021.

Avila-Alonso, D., Baetens, J.M., Cardenas, R., De Baets, B: Oceanic response to the consecutive Hurricanes Dorian and Humberto (2019) in the Sargasso Sea, Nat. Hazards Earth Syst. Sci., 21(2): 837-859, https://doi.org/10.5194/nhess-21-837-2021, 2021.

Babanin, A.V., Rogers, W.E., de Camargo, R: Waves and Swells in High Wind and Extreme Fetches, Measurements in the Southern Ocean, Front. Mar. Sci., 6:361, doi: 10.3389/fmars.2019.00361, 2019.

Bethel, B.J., Dong, C., Zhou, S., Cao, Y: Bidirectional Modeling of Surface Winds and Significant Wave Heights in the

https://doi.org/10.5194/os-2021-84
Preprint. Discussion started: 8 September 2021

Caribbean Sea. J. Mar. Sci. Eng., 9(5), 547, https://doi.org/10.3390/jmse9050547, 2021.

Bhalachandran, S., Nadimpalli, R., Osuri, K.K., Marks Jr., F.D., Gopalakrishnan, S., Subramanian, S., Mohanty, U.C., Niyogi, D: On the processes influencing rapid intensity changes of tropical cyclones over the Bay of Bengal. Sci. Rep., 9, 3382, https://doi.org/10.1038/s41598-019-40332-z, 2019.

Campos, R.M., Costa, M.O., Almeida, F., Guedes Soares, C: Operational Wave Forecast Selection in the Atlantic Ocean Using Random Forests. J. Mar. Sci. Eng., 9(3), 298, https://doi.org/10.3390/jmse9030298, 2021.

Cecilio, R.O., Dillenburg, S.R: An ocean wind-wave climatology for the Southern Brazilian Shelf. Part 1: Problem presentation and model validation, Dyn. Atmospheres Oceans, 89: 101101, https://doi.org/10.1016/j.dynatmoce.2019.101101, 2020.

Chao, Y., Huang, H., Wang, D., Liu, Y., Guo, Z: The Characteristics of Storm Wave Behavior and Its Effect on Cage Culture Using the ADCIRC+SWAN Model in Houshui Bay, China. J. Ocean Univ. of China, 19(2), 307-319, DOI: 10.1007/s11802-020-3941-3, 2020.

Chen, T.: Probabilistic forecasting of coastal wave height during typhoon warning period using machine learning methods, Hydroinformatics, 21(2), 343-358, https://doi.org/10.2166/hydro.2019.115, 2019.

Chen, S., Wang, Y: Improving Coastal Ocean Wave Height Forecasting during Typhoons by using Local Meteorological and Neighboring Wave Data in Support Vector Regression Models, J. Mar. Sci. Eng., 8(3), 149, https://doi.org/10.3390/jmse8030149, 2020.

Chen, J., Pillai, A.C., Johanning, L., Ashton, I.: Using machine learning to derive spatial wave data: A case study for a marine energy site, Environ. Model. Softw., 142: 105066, https://doi.org/10.1016/j.envsoft.2021.105066, 2021.

Chen, Y., Gao, S., Li, X., Shen, X: Key Environmental Factors for Rapid Intensification of the South China Sea Tropical Cyclones, Front. Earth Sci., 8:609727, doi: 10.3389/feart.2020.609727, 2021.

Cheriton, O.M., Storlazzi, C.D., Rosenberger, K.J., Sherman, C.E., Schmidt, W.E: Rapid observations of ocean dynamics and stratification along a steep island coast during Hurricane María, Sci. Adv., 7(20), DOI: 10.1126/sciadv.abf1552, 2021.

Choi, J.K., Lee, B: Combining LSTM Network Ensemble via Adaptive Weighting for Improved Time Series Forecasting, Math. Probl. Eng., 2470171, https://doi.org/10.1155/2018/2470171, 2018.

Collins, C., Hesser, T., Rogowski, P., Merrifield, S: Altimeter Observations of Tropical Cyclone-generated Sea States: Spatial Analysis and Operational Hindcast Evaluation, J. Mar. Sci. Eng., 9(2), 216, https://doi.org/10.3390/jmse9020216, 2021.

Constantin, A.: Nonlinear water waves: introduction and overview, Philos. Trans. A Math. Phys. Eng. Sci., 376(2111), L 20170310. doi: 10.1098/rsta.2017.0310, 2018.

Fan, S., Xiao, N., Dong, S: A novel model to predict SWH based on long short-term memory network, Ocean Eng., 205: 107298, https://doi.org/10.1016/j.oceaneng.2020.107298, 2020.

Gao, S., Huang, J., Liu, G, Bi, F., Bai, Z: A forecasting model for wave heights based on a long short-term memory neural network, Acta Oceanologica Sinica, 40, 62-69, https://doi.org/10.1007/s13131-020-1680-3, 2021.

Golbazi, M., Archer, C.L: Methods to Estimate Surface Roughness for Offshore Wind Energy, Adv. Meteorol., 2019(2), 1-15, https://doi.org/10.1155/2019/5695481, 2019.

Guan, X.: Wave height prediction based on CNN-LSTM. 2020 2nd International Conference on Machine Learning, Big Data and Business Intelligence (MLBDBI), 23-25 Oct 2020, Taiyuan, China, DOI: 10.1109/MLBDBI51377.2020.00009, 2020.

https://doi.org/10.5194/os-2021-84
Preprint. Discussion started: 8 September 2021

Guo, Y., Hou, Y., Liu, Z., Du, M: Risk Prediction of Coastal Hazards Induced by Typhoon: A Case Study in the Coastal Region of Shenzhen, China, Remote Sens., 12(11), 1731, https://doi.org/10.3390/rs12111731, 2020.

Hatzikyriakou, A., Lin, N: Simulating storm surge waves for structural vulnerability estimation and flood hazard mapping, Nat. Hazard, 89, 939-962, https://doi.org/10.1007/s11069-017-3001-5, 2017.

Haryanto, Y.D., Riama, N.F., Purnama, D.R., Sigalingging, A.D: The Effect of the Difference in Intensity and Track of Tropical Cyclone on Significant Wave Height and Wave Direction in the Southeast Indian Ocean, The World Scientific Journal, 5492048, https://doi.org/10.1155/2021/5492048, 2021.

Hochreiter, S., Schmidhuber, J: Long Short-term Memory, Neural Computation, 9(8), 1735-1780, https://doi.org/10.1162/neco.1997.9.8.1735, 1997.

Hu, Y., Shao, W., Wei, Y., Zuo, J: Analysis of Typhoon-Induced Waves along Typhoon Tracks in the Western North Pacific Ocean, 1998-2017, J. Mar. Sci. Eng., 8(7), 521, https://doi.org/10.3390/jmse8070521, 2020.

Hu, H., van der Westhuysen, A.J., Chu, P., Fujisaki-Manome, A: Predicting Lake Erie wave heights and periods using XGBoost and LSTM, Ocean Model., 164: 101832, https://doi.org/10.1016/j.ocemod.2021.101832, 2021.

Huang, W., Dong, S: Improved short-term prediction of SWH by decomposing deterministic and stochastic components, Renew. Energy, 177, 743-758. https://doi.org/10.1016/j.renene.2021.06.008, 2021.

Hwang, P.A., Fan, Y: Effective Fetch and Duration of Tropical Cyclone Wind Fields Estimated from Simultaneous Wind and Wave Measurements: Surface Wave and Air-Sea Exchange Computation, J. Phys. Ocean., 47(2), 447-470. https://doi.org/10.1175/JPO-D-16-0180.1, 2017.

Jörges, C., Berbenbrink, C., Stumpe, B: Prediction and reconstruction of ocean wave heights based on bathymetric data using LSTM neural networks, Ocean Eng., 232: 109046, https://doi.org/10.1016/j.oceaneng.2021.109046, 2021.

Joyce, B.R., Gonzalez-Lopez, J., Van der Westhuysen, A.J., Yang, D., Pringle, J., Westerink, J.J., Cox, A.T: U.S. IOOS Coastal and Ocean Modeling Testbed: Hurricane-Induced Winds, Waves, and Surge for Deep Ocean, Reef-Fringed Islands in the Caribbean, J. Geophys. Res. Ocean, 124(4), 2876-2907, https://doi.org/10.1029/2018JC014687, 2019.

Kaloop, M.R., Beshr, A.A.A., Zarzoura, F., Ban, W.H., Hu, J.W: Predicting lake wave height based on regression classification and multi input-single output soft computing models,Arab. J. Geosci., 13: 591, https://doi.org/10.1007/s12517-020-05498-1, 2020.

Karniadakis, G.E., Kevrekidis, I.G., Lu, L., Perdikaris, P., Wang, S., Yang, L: Physics-informed machine learning, Nat. Rev. Phys., 3, 422-440, https://doi.org/10.1038/s42254-021-00314-5, 2021.

Kashinath, K., Mustafa, M., Albert, A: Physics-informed machine learning: case studies for weather and climate modelling, Phil. Trans. R. Soc. A., 3792020009320200093. http://doi.org/10.1098/rsta.2020.0093, 2021.

Khodkar, M.A., Hassanzadeh, P: A data-driven, physics-informed framework for forecasting the spatiotemporal evolution of chaotic dynamics with nonlinearities modeled as exogenous forcing, J. Comput. Phys., 440: 110412, https://doi.org/10.1016/j.jcp.2021.110412, 2021.

Kim, K., Lee, J., Roh, M., Han, K., Lee, G: Prediction of Ocean Weather Based on Denoising AutoEncoder and Convolutional LSTM, J. Mar. Sci. Eng., 8(10), 805, https://doi.org/10.3390/jmse8100805, 2020.

Köllisch, N., Behrendt, J., Klein, M., Hoffmann, N: Nonlinear real time prediction of ocean surface waves, Ocean Eng., 157, 387-400, https://doi.org/10.1016/j.oceaneng.2018.03.048, 2018.

https://doi.org/10.5194/os-2021-84
Preprint. Discussion started: 8 September 2021

Leroux, D., Wood, K., Elsberry, R.L., Cayanan, E.O., Hendricks, E., Kucas, M., Otto, P., Rogers, R., Sampson, B., Yu, Z: Recent Advances in Research and Forecasting of Tropical Cyclone Track, Intensity, and Structure at Landfall, Tropic. Cyclone Res. Rev., 7(2), 85-105, https://doi.org/10.6057/2018TCRR02.02, 2018.

Li, M., Liu, K: Probabilistic Prediction of SWH Using Dynamic Bayesian Network and Information Flow, Water, 12(8), 2075, https://doi.org/10.3390/w12082075, 2020.

Li, M., Zhang, R., Liu, K: A New Marine Disaster Assessment Model Combining Bayesian Network with Information Diffusion, J. Mar. Sci. Eng., 9(6), 640, https://doi.org/10.3390/jmse9060640, 2021.

Liu, L.L., Wang, W., Huang, R.X: The Mechanical Energy Input to the Ocean Induced by Tropical Cyclones, J. Phys. Ocean., 38(6), 1253-1266, https://doi.org/10.1175/2007JPO3786.1, 2008.

Marsooli, R., Lin, N: Numerical Modeling of Historical Storm Tides and Waves and Their Interactions Along the U.S. East and Gulf Coasts, J. Geophys. Res. Ocean, 123, 3844-3874, https://doi.org/10.1029/2017JC013434, 2018.

Masoomi, H., van de Lindt, J.W., Ameri, M.R., Do, T., Webb, B: Combined Wind-Wave-Surge Hurricane-Induced Damage Prediction for Buildings, J. Struct. Eng., 145(1), https://doi.org/10.1061/(ASCE)ST.1943-541X.0002241, 2018.

Meng, F., Song, T., Xu, D., Xie, P., Li, Y: Forecasting tropical cyclone wave height using bidirectional gated recurrent unit, Ocean Eng., 234, 108795, https://doi.org/10.1016/j.oceaneng.2021.108795, 2021.

Niaki, S.A., Haghighat, E., Campbell, T., Poursartip, A., Vaziri, R: Physics-informed neural network for modelling the thermochemical curing process of composite-tool systems during manufacture, Comput. Methods Appl. Mech. Eng., 384: 113959, https://doi.org/10.1016/j.cma.2021.113959, 2021.

Pushkarev, A.N., Zakharov, V.E: Nonlinear amplification of ocean waves in straits, Theor. Math. Phys., 203, 535-546, https://doi.org/10.1134/S0040577920040091, 2020.

Pushpam, P.M.M., Enigo, F.V.S: Forecasting SWH using RNN-LSTM Models. 2020 4^{th} International Conference on Intelligent Computing and Control Systems (ICICCS), 13-15 May 2020. Madurai, India, DOI: 10.1109/ICICCS48265.2020.9121040, 2020.

Qiao, C., Myers, A.T: Modeling Spatio-Temporal Characteristics of Metocean Conditions During Hurricanes Using Deep Neural Networks. ASME 2020 39^{th} International Conference on Ocean, Offshore and Arctic Engineering, August 3-7, https://doi.org/10.1115/OMAE2020-18989, 2020.

Qiao, C., Myers, A.T: Surrogate modeling of time-dependent metocean conditions during hurricanes, Nat. Hazards, https://doi.org/10.1007/s11069-021-05002-2, 2021.

Raj, N., Brown, J: An EEMD-BiLSTM Algorithm Integrated with Boruta Random Forest Optimiser for SWH Forecasting along Coastal Areas of Queensland, Australia, Remote Sens., 13(8), 1456, https://doi.org/10.3390/rs13081456, 2021.

Rollano, F.T., Brown, A., Ellenson, A: Breaking waves in deep water: measurements and modeling of energy dissipation, Ocean Dyn., 69, 1165-1179, https://doi.org/10.1007/s10236-019-01301-2, 2019.

Sahoo, B., Jose, F., Bhaskaran, P.K: Hydrodynamic response of Bahamas archipelago to storm surge and hurricane generated waves – A case study for Hurricane Joaquin, Ocean Eng., 184, 227-238, https://doi.org/10.1016/j.oceaneng.2019.05.026, 2019.

Sahoo, B., Sahoo, T., Bhaskaran, P.K: Wave-current-surge interaction in a changing climate over a shallow continental shelf region, Reg. Stud. Mar. Sci, 46: 101910, https://doi.org/10.1016/j.rsma.2021.101910, 2021.

https://doi.org/10.5194/os-2021-84
Preprint. Discussion started: 8 September 2021

Shao, Z., Liang, B., Li, H., Li, P., Lee, D: Extreme SWH of tropical cyclone waves in the South China Sea, Nat. Hazards Earth Syst. Sci., 19, 2067-2077, https://doi.org/10.5194/nhess-19-2067-2019, 2019.

Sharifineyestani, E., Tahvildari, N: Nonlinear Wave Evolution in Interaction with Currents and Viscoleastic Muds, J. Mar. Sci. Eng., 9(5), 529, https://doi.org/10.3390/jmse9050529, 2021.

Song, H., Kuang, C., Gu, J., Zou, Q., Liang, H., Sun, X., Ma, Z: Nonlinear tide-surge-wave interaction at a shallow coast with large scale sequential harbor constructions, Estuar. Coast. Shelf Sci, 233: 106543, https://doi.org/10.1016/j.ecss.2019.106543, 2020.

Tamizi, A., Young, I.R: The Spatial Distribution of Ocean Waves in Tropical Cyclones, J. Phys. Ocean., 50(8), 2123-2139, https://doi.org/10.1175/JPO-D-20-0020.1, 2020.

Tamizi, A., Alves, J., Young, I.R: The Physics of Ocean Wave Evolution within Tropical Cyclones, J. Phys. Ocean, 51(7), 2373-2388, https://doi.org/10.1175/JPO-D-21-0005.1, 2021.

Tian, D., Zhang, H., Zhang, W., Zhou, F., Sun, X., Zhou, Y., Ke, D: Wave Glider Observations of Surface Waves During Three Tropical Cyclones in the South China Sea, Water, 12(5), 1331, https://doi.org/10.3390/w12051331, 2020.

Wang, X., Yao, C., Gao, G., Jiang, H., Xu, D., Chen, G., Zhang, Z: Simulating tropical cyclone waves in the East China Sea with an event-based, parametric-adjusted model, J. Ocean., 76, 439-457, https://doi.org/10.1007/s10872-020-00555-5, 2020.

Wang, J., Wang, Y., Yang, J: Forecasting of SWH Based on Gated Recurrent unit Network in the Taiwan Strait and Its Adjacent Waters, Water, 13(1), 86, https://doi.org/10.3390/w13010086, 2021.

Wei, C., Cheng, J: Nearshore two-step typhoon wind-wave prediction using deep recurrent neural networks, Hydroinformatics, 22(2), 346-367, https://doi.org/10.2166/hydro.2019.084, 2020.

Wei, Z: Forecasting wind waves in the US Atlantic Coast using an artificial neural network model: Towards an AI-based storm forecast system, Ocean Eng., 237: 109646, https://doi.org/10.1016/j.oceaneng.2021.109646, 2021.

Wu, M., Stefanakos, C., Gao, Z: Multi-Step-Ahead Forecasting of Wave Conditions Based on a Physics-Based Machine Learning (PBML) Model for Marine Operations, J. Mar. Sci. Eng., 8(12), 992, https://doi.org/10.3390/jmse8120992, 2020.

Yim, S.C., Osborne, A.R., Mohtat, A: Nonlinear Ocean Wave Models and Laboratory Simulation of High Seastates and Rogue Waves. Proceedings of the ASME 2017 International Conference on Ocean, Offshore and Arctic Engineering, OMAE2017, June 25-30, 2017. Trondheim, Norway, https://doi.org/10.1115/OMAE2017-62706, 2017.

Yu, Y., Si, X., Hu, C., Zhang, J: A Review of Recurrent Neural Networks: LSTM Cells and Networks, Neural Comput., 31, 1235-1270, https://doi.org/10.1162/neco_a_01199, 2019.

Zhang, L., Oey, L: An Observational Analysis of Ocean Surface Waves in Tropical Cyclones in the Western North Pacific Ocean, J. Geophys. Res.: Ocean, 124(1), 184-195, https://doi.org/10.1029/2018JC014517, 2018.

Zhang, C., Li, C: Effects of hurricane forward speed and approach angle on storm surges: an idealized numerical experiment. Acta. Oceanol. Sin., 38, 48-56. https://doi.org/10.1007/s13131-018-1081-z, 2019.

Zhang, Z., Rai, R., Chowdhury, S., Doermann, D: MIDPhyNet: Memorized Infusion of Decomposed Physics in Neural Networks to Model Dynamic Systems, Neurocomputing, 428, 116-129, https://doi.org/10.1016/j.neucom.2020.11.042, 2020.

Zhao, K., Wang, J: SWH forecasting based on the hybrid EMD-SVM method, Indian J. Geo Mar. Sci., 48(12), 1957-1962, 2018.

https://doi.org/10.5194/os-2021-84
Preprint. Discussion started: 8 September 2021

Zhou, S., Bethel, B.J., Sun, W., Zhao, Y., Xie, W., Dong, C: Improving SWH Forecasts Using a Joint Empirical Mode Decomposition-Long Short-Term Memory Network, J. Mar. Sci. Eng., 9, 744, 2021a.

Zhou, S., Xie, W., Lu, Y., Wang, Y., Zhou, Y., Hui, N., Dong, C: ConvLSTM-Based Wave Forecasts in the South and East China Seas, Front. Mar. Sci., 8:680079. doi: 10.3389/fmars.2021.680079, 2021b.

Zobeiry, N., Humfeld, K.D: A physics-informed machine learning approach for solving heat transfer equation in advanced manufacturing and engineering applications, Eng. Appl. AI, 101: 104232, https://doi.org/10.1016/j.engappai.2021.104232, 2021.

Zubier, K: Using an Artificial Neural Network for Wave Height Forecasting in the Red Sea, Indian J. Geo Mar. Sci, 49(2), 184-191, 2020.